

ON PRESSURE GRADIENTS AND RAPID MIGRATION OF SOLIDS IN A NONUNIFORM SOLAR NEBULA

NADER HAGHIGHIPOUR AND ALAN P. BOSS

Department of Terrestrial Magnetism, Carnegie Institution of Washington, 5241 Broad Branch Road, Washington, DC 20015;
nader@dtm.ciw.edu, boss@dtm.ciw.edu

Received 2002 July 16; accepted 2002 October 9

ABSTRACT

We study the motions of small solids, ranging from micron-sized dust grains to 100 m objects, in the vicinity of a local density enhancement of an isothermal gaseous solar nebula. Being interested in possible application of the results to the formation of planetesimals in the vicinity of clumps and spiral arms in a circumstellar disk, we numerically integrate the equations of motion of such solids and study their migrations for different values of their sizes and masses and also for different physical properties of the gas, such as its density and temperature. We show that, considering the drag force of the gas, it is possible for solids, within a certain range of size and mass, to migrate rapidly (i.e., within ~ 1000 yr) toward the location of a local maximum density, where collisions and coagulation may result in an accelerated rate of planetesimal formation.

Subject headings: planetary systems: formation — planetary systems: protoplanetary disks — solar system: formation

1. INTRODUCTION

It is generally believed that planet formation starts as a secondary process to star formation by coalescence of small bodies in circumstellar disks. With regard to our solar system, two mechanisms have been proposed for the formation of the giant planets in such a disk around our Sun: the widely accepted core accretion model (Pollack et al. 1996), and the disk instability scenario (Boss 2000). It has recently been noted that a solar nebula massive enough to possibly form giant planets via the core accretion model is likely marginally gravitationally unstable (Pollack et al. 1996; Boss 2000). The alternative approach, namely, the disk instability mechanism, however, implies that such an instability could lead to rapid formation of gas giant planets. It is therefore of great importance to study how the dynamics of small solids will be affected in such an unstable environment and what implications there will be on the collision and coagulation process.

In general, in a rotating nonturbulent gaseous disk at hydrostatic equilibrium, there is a radial gradient associated with the gas pressure. This pressure gradient counteracts the gravitational attraction of the central star and causes the gas molecules to have slightly different velocities than Keplerian circular. When the pressure gradient is positive, the velocity of a gas molecule is greater than the local Keplerian velocity. A solid in the gas, in this case, feels an acceleration by the gas along its orbit, and consequently, the increase in its orbital angular momentum forces the solid to a larger orbit. In this case, we say that the solid feels a “tail wind.” The opposite is true when the pressure gradient is negative. That is, a solid body will be subject to a “head wind” and will migrate toward smaller orbits.

One of the features of a rotating gravitationally unstable disk is the appearance of spiral arms or clumps where the density of the medium is locally enhanced. In the vicinity of such density enhancements, the pressure of the gas may

change radially and cause the particles in the disk to migrate toward the location of the maximum gas density. We are interested in studying the dynamics of solids that undergo such migration and in exploring the possibility of applying the results to the formation of planetesimals in a marginally gravitationally unstable disk. As the first stage of our project, we present here the results of a systematic study of the migration of solids subject to gas drag, around the location of the maximum density of a circumstellar disk. To focus attention on the dynamics of the solids and its association with parameters such as the temperature of the gas, the sizes of the objects, and also the values of their densities, we consider a hypothetical solar nebula with a circularly symmetric density function.

Studies of the motions of solids in gaseous mediums have been presented by many authors. In a detailed analytical analysis, Kiang (1962) studied the dynamical evolution of solids in elliptical orbits subject to resistive forces proportional to arbitrary powers of their relative velocities with respect to the medium and also their distances to the star. In his study, Kiang considered three cases of stationary, uniformly rotating, and also freely rotating gaseous mediums. However, he did not consider the pressure gradient of the gas. It was Whipple (1964) who first mentioned that the rotation of the solar nebula deviates from Keplerian because of counterbalancing the gravity of the Sun by the internal pressure of the gas, which in turn results in inward/outward migration of small solids. Whipple (1972) studied the dynamics of such solids in the solar nebula, where, following an approximation by Probst & Fassio (1969), he also included the resistive effect of the gas. Whipple’s work was subsequently expanded on and generalized by Weidenschilling (1977) for a variety of model nebulae and different sizes of solids.

A comprehensive study of the effect of gas drag on the motions of solid bodies can also be found in the classic work of Adachi, Hayashi, & Nakazawa (1976). In their paper,

Adachi et al. (1976) studied the motion of a solid on an elliptical orbit in a solar nebula whose density and temperature vary inversely with different powers of the distance from the Sun. They also presented a detailed analysis of the form of the gas drag for different relative velocities and relative sizes of solids, and also for different values of the gas Reynolds number.

Among the studies of the dynamical evolution of solids in a gaseous disk, one can cite Weidenschilling & Davis (1985) and also Kary, Lissauer, & Greenzweig (1993) for their papers on the study of the orbital dynamics of planetesimals near a planet in a resistive medium, Malhotra (1993) for her study of the resonance capture of planetesimals subject to a drag force proportional to their velocities relative to the gas as a barrier for the inward flow of solids to the accretion zone of a planetary embryo in the solar nebula, Supulver & Lin (2000) for their paper on the formation of icy planetesimals subject to a linear combination of Stokes and Epstein drags in an azimuthally symmetric, turbulent, and thin solar nebula with a polytropic equation of state, and also Iwasaki, Tanaka, & Emori (2001) for studying the stability/instability of protoplanets subject to gas drag.

In this paper, we study the dynamics of solid bodies in a nonuniform gaseous disk. Our model nebula consists of a Sun-like star at its center and noninteracting collisionless bodies scattered on its midplane. We also consider the effect of the drag force of the nebula.

The outline of this paper is as follows. Section 2 introduces the equations of motion and also the basic relations concerning the drag force of the gas. Section 3 defines the system of interest, and § 4 presents the results of our numerical simulations. Section 5 concludes this study by reviewing the results and discussing their applications.

2. BASIC RELATIONS

We consider a thin and isothermal gaseous disk with a Sun-like star at rest, at the center of its midplane. A solid object in this medium, in addition to the gravitational force of the central star, is also subject to gas drag. In an inertial coordinate system with its origin at the position of the star and its axes on the midplane of the nebula, the equation of motion of such a solid can be written as

$$m_p \ddot{\mathbf{r}}_p = -GMm_p \left(\frac{\mathbf{r}_p}{r_p^3} \right) + \mathbf{F}_{\text{drag}} , \quad (1)$$

where m_p and \mathbf{r}_p represent the mass and the position vector of the solid, M is the mass of the central star, and G is the gravitational constant. The quantity \mathbf{F}_{drag} in equation (1) denotes the drag force of the nebula.

2.1. Gas Drag

In general, the drag force of a gaseous medium with a density $\rho_g(\mathbf{r})$ on a spherical body with radius a_p is proportional to the square of the relative velocity of the body with respect to the gas, \mathbf{V}_{rel} , and is given by (Landau & Lifshitz 1959; Adachi et al. 1976)

$$\mathbf{F}_{\text{drag}} = -\frac{1}{2} C_D \pi a_p^2 \rho_g(\mathbf{r}_p) v_{\text{rel}} \mathbf{V}_{\text{rel}} . \quad (2)$$

In this equation, $v_{\text{rel}} = |\mathbf{V}_{\text{rel}}|$ and $\mathbf{V}_{\text{rel}} = \mathbf{V}_p - \mathbf{V}_g$, where \mathbf{V}_p is the velocity of the body and \mathbf{V}_g , the velocity of the gas at

the location of the body, has a magnitude given by

$$v_g^2 = \frac{GM}{r_p} + \frac{r_p}{\rho_g(\mathbf{r}_p)} \left(\frac{d\mathcal{P}_g}{dr} \right)_{r=r_p} . \quad (3)$$

In this equation, \mathcal{P}_g is the pressure of the gas. As shown in equation (3), the velocity of the gas differs slightly from its Keplerian circular value (first term of the right-hand side) due to the pressure gradient.

The quantity C_D in equation (2) is the drag coefficient, which is a dimensionless constant that depends on the gas Reynolds number, the ratio of v_{rel} to the speed of sound in the medium (the Mach number), and also the relative size of the solid compared to the mean free path of the gas molecules (the Knudsen number). For a detailed analysis of the drag coefficient, we refer the reader to Adachi et al. (1976).

For the cases in which the mean free path of the gas molecules is smaller than the size of the object, we have (Whipple 1972; Weidenschilling 1977)

$$C_D \simeq \begin{cases} 24 \text{Re}^{-1} & \text{if } \text{Re} < 1 \text{ (Stokes drag)} , \\ 24 \text{Re}^{-0.6} & \text{if } 1 < \text{Re} < 800 , \\ 0.44 & \text{if } \text{Re} > 800 , \end{cases} \quad (4)$$

where Re is the gas Reynolds number. For a gas with a viscosity ν ,

$$\text{Re} = \frac{2}{\nu} \rho_g(\mathbf{r}_p) a_p v_{\text{rel}} , \quad (5)$$

and

$$\nu = \frac{1}{3} \left(\frac{m_0 \bar{v}_{\text{th}}}{\sigma} \right) , \quad (6)$$

where m_0 and \bar{v}_{th} represent the mass and the mean thermal velocity of the gas molecules and σ is their collisional cross section (Adachi et al. 1976; Weidenschilling 1977).

For particles moving much slower than the gas mean thermal velocity and with sizes smaller than the mean free path of the gas molecules, \mathbf{F}_{drag} can be approximately written as

$$\mathbf{F}_{\text{drag}} = -\frac{4}{3} \pi \rho_g(\mathbf{r}_p) a_p^2 \bar{v}_{\text{th}} \mathbf{V}_{\text{rel}} . \quad (7)$$

Equation (6) is known as Epstein drag (Kennard 1938; Epstein 1924).

As shown by equations (2) and (7), the resistive force of the gas varies by the size of the object. Anticipating numerically integrating equation (1) for different values of a_p , we follow Supulver & Lin (2000) and combine equations (2) and (7) by introducing $f = a_p/(a_p + l)$, where l is the mean free path of the gas molecules. We now write

$$\mathbf{F}_{\text{drag}} = -\frac{4}{3} \pi a_p^2 \rho_g(\mathbf{r}_p) [(1-f)\bar{v}_{\text{th}} + \frac{3}{8} f C_D v_{\text{rel}}] \mathbf{V}_{\text{rel}} , \quad (8)$$

which is particularly useful for transitional cases in which the size of solids and the mean free path of the gas molecules are comparable.

2.2. Equation of Motion

The equation of motion of a solid in this study is given by equation (1). For the purpose of numerical integrations, it is more convenient to write this equation in a dimensionless form. Introducing the quantities r_0 and t_0 , which carry the

dimensions of length and time, respectively, equation (1) can be written as

$$\ddot{\hat{\mathbf{r}}} = -\hat{k} \left(\frac{\hat{\mathbf{r}}}{\hat{r}^3} \right) + \hat{\mathbf{F}}_{\text{drag}}, \quad (9)$$

where $\mathbf{r}_p = r_0 \hat{\mathbf{r}}$, $t = t_0 \hat{t}$, $\hat{k} = GMt_0^2/r_0^3$, and $\hat{\mathbf{F}}_{\text{drag}} = t_0^2 \mathbf{F}_{\text{drag}}/m_p r_0$. We choose r_0 and t_0 such that $\hat{k} = 1$. For a solid restricted to move on the midplane of the nebula, equation (9), in a dimensionless form and in a plane-polar coordinate system with axes on the midplane of the disk, is written as

$$P_r = \dot{r}, \quad (10)$$

$$P_\theta = r^2 \dot{\theta}, \quad (11)$$

$$\dot{P}_r = \frac{1}{r^3} P_\theta^2 - \frac{1}{r^2} - \frac{4}{3} \pi \hat{a}_p^2 \hat{\rho}_g(r) P_r \left[(1-f) \hat{v}_{\text{th}} + \frac{3}{8} f C_D \hat{v}_{\text{rel}} \right], \quad (12)$$

$$\dot{P}_\theta = -\frac{4}{3} \pi r \hat{a}_p^2 \hat{\rho}_g(r) (\hat{v}_{\text{rel}}^2 - P_r^2)^{1/2} \left[(1-f) \hat{v}_{\text{th}} + \frac{3}{8} f C_D \hat{v}_{\text{rel}} \right], \quad (13)$$

where P_r and P_θ are, respectively, the dimensionless radial and angular momenta of the solid, $\hat{\rho}_g(r) = r_0^3 \rho_g(r)/m_p$, $\hat{v}_{\text{rel}} = v_{\text{rel}} t_0/r_0$, and $\hat{a}_p = a_p/r_0$. In equations (10)–(13), the hat signs for all other quantities have been dropped for simplicity.

In writing the equations of motions of solids as in equations (10)–(13), the relative velocity \mathbf{V}_{rel} has been resolved into dimensionless radial and transverse components as

$$\left(\frac{t_0 \mathbf{V}_{\text{rel}}}{r_0} \right)_{\text{radial}} = \dot{r},$$

$$\left(\frac{t_0 \mathbf{V}_{\text{rel}}}{r_0} \right)_{\text{transverse}} = r \dot{\theta} + \left[\frac{1}{r} - \frac{r}{\hat{\rho}_g(r)} \frac{d\hat{\mathcal{P}}_g}{dr} \right]^{1/2}, \quad (14)$$

where $\hat{\mathcal{P}}_g = \mathcal{P}_g r_0 t_0^2/m_p$ is the dimensionless pressure of the gas. The dimensionless magnitude of \mathbf{V}_{rel} is therefore given by

$$\hat{v}_{\text{rel}}^2 = P_r^2 + \left\{ \frac{P_\theta}{r} + \left[\frac{1}{r} - \frac{r}{\hat{\rho}_g(r)} \frac{d\hat{\mathcal{P}}_g}{dr} \right]^{1/2} \right\}^2. \quad (15)$$

For small particles, the magnitude of \hat{v}_{rel} is dominated by the magnitude of its radial component, whereas for large objects, it is the transverse components of their velocities relative to the gas that have considerable contributions in equation (15). Also, as shown in equation (12), it is the radial component of the relative velocity that is important for the radial migration of solids. The effect of the transverse component of the relative velocity appears in the changes of the angular momenta of solids (eq. [13]), which can have important contributions when accretion is taken into consideration.

3. THE PHYSICAL MODEL

We consider a gaseous nebula of pure molecular hydrogen with a uniform temperature T and a density given by

$$\hat{\rho}_g(r) = \hat{\rho}_0 e^{-\beta(r/r_m-1)^2}. \quad (16)$$

In equation (16), $\hat{\rho}_0 = r_0^3 \rho_0/m_p$, where ρ_0 is the magnitude of the local maximum of the density. The quantities r and r_m in

this equation are dimensionless, and the coefficient β is a positive constant. Figure 1 shows $\hat{\rho}_g(r)$ for $\beta = 0.5$ and 1. For such isothermal nebula with a density given by equation (16), the nebula's surface density varies as $r^{3/2}$ times the density of the midplane.

It is necessary to emphasize that the choice of density, as given by equation (16), has been made solely to focus attention on the effects of the pressure gradient and gas drag of the disk on migration of solids on both sides of the location of the maximum density. In a more realistic system, in particular at the presence of spiral arms and clumps, the density of the gas will have a much more complicated form. Extension of this work to such cases is the subject of upcoming articles.

As mentioned earlier, we would like to study the dynamics of a solid in a gaseous disk with a density given by equation (16) by numerically simulating its motion given by equations (10)–(13). These equations require us to write certain quantities, such as the pressure of the gas, its mean thermal velocity, the mean free path of its molecules, and also the velocity of a solid relative to the gas, in terms of the gas density $\hat{\rho}_g(r)$. To do so, we assume that our model nebula obeys the equation of state of an ideal gas, $\mathcal{P}_g = nk_B T$, where n is the gas number density and k_B is the Boltzmann's constant. The dimensionless mean thermal velocity of the gas molecules is therefore given by

$$\hat{v}_{\text{th}}^2 = \frac{8k_B r_0 T}{\pi G M m_0}. \quad (17)$$

Substituting for T from the ideal gas law in equation (17), the dimensionless pressure of the gas will be equal to

$$\hat{\mathcal{P}}_g = \frac{1}{8} \pi \hat{v}_{\text{th}}^2 \hat{\rho}_g(r). \quad (18)$$

Substituting for $\hat{\mathcal{P}}_g$ from equation (18) in equation (15), the relative velocity of a solid with respect to the gas can be written as

$$\hat{v}_{\text{rel}}^2 = P_r^2 + \left\{ \frac{P_\theta}{r} - \left[\frac{1}{r} + \frac{\pi r \hat{v}_{\text{th}}^2}{8 \hat{\rho}_g(r)} \frac{d\hat{\rho}_g(r)}{dr} \right]^{1/2} \right\}^2. \quad (19)$$

The mean free path of the gas molecules can also be written in terms of the gas density. Recall that the quantity f in equation (8), as defined in § 2.2, is dimensionless by definition. It is therefore not necessary in calculation of l to consider dimensionless quantities. Assuming a diameter of a_0 for the gas molecules, $l = 1/(\pi a_0^2 n)$. From the ideal gas law, one can write

$$l = \frac{m_0}{\pi a_0^2 \rho_g(r)}. \quad (20)$$

For molecular hydrogen, $a_0 = 1.5 \times 10^{-8}$ cm. The mean free path of the molecules of our model nebula can therefore be written as l (cm) = $4.72 \times 10^{-9}/\rho_g(r)$ (g cm $^{-3}$).

4. NUMERICAL SIMULATIONS

We consider a gas density given by equation (16) with a peak equal to 10^{-9} g cm $^{-3}$ at 1 AU. The value of β is considered as a parameter in our simulations. As mentioned in § 3, we choose our units such that $\hat{k} = 1$. Therefore, the quantities r_0 and t_0 are related as $t_0^2 = r_0^3/GM$. Introducing a new

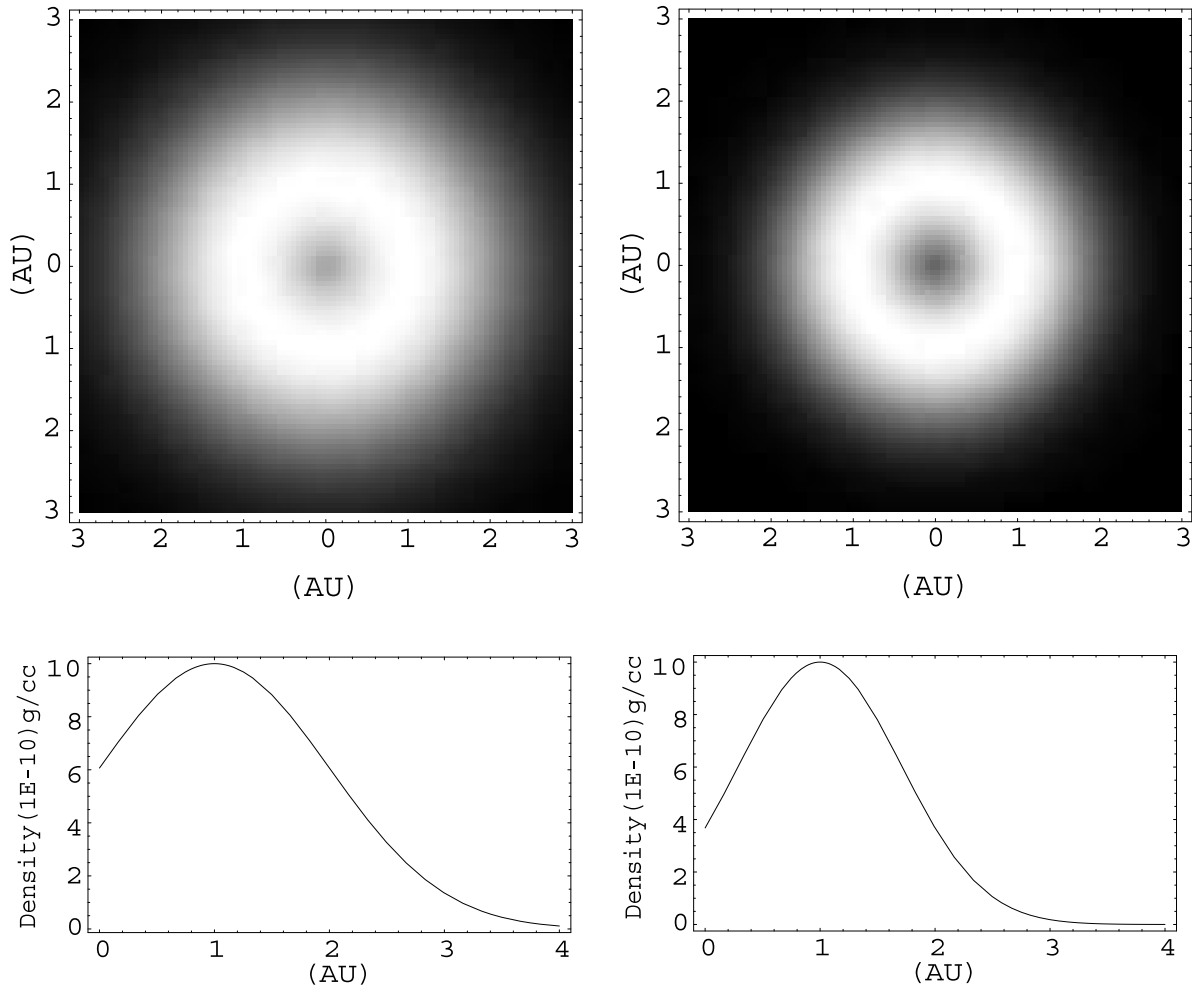


FIG. 1.—Graphs of the density of the gas for $\beta = 0.5$ (left) and $\beta = 1$ (right) in the disk midplane

variable $T_0 = 2\pi t_0$, we have

$$T_0 = 2\pi \left(\frac{r_0^3}{GM} \right)^{1/2}. \quad (21)$$

Equation (21) implies that T_0 can be considered as the period of an object rotating uniformly around the star M on a circular path with radius r_0 . In our physical model, an object at $r = r_m$ has such a uniform circular motion. With the location of the maximum density at 1 AU, we can now consider $r_0 = 1$ AU, which implies r_m is equal to unity and therefore, from equation (21), $t_0 \simeq 5.03 \times 10^6$ s $\simeq 0.16$ yr.

Another important quantity that has to be determined at the start of our simulations is the drag coefficient C_D . For the values of Re smaller than 800, the magnitude of C_D varies with the position and the velocity of the object through its dependence on the gas Reynolds number (eq. [4]). Note that for the density function of equation (16), the magnitude of the velocity of an object relative to the gas, as given by equation (19), can be written as

$$\hat{v}_{rel}^2 = P_r^2 + \left\{ \frac{P_\theta}{r} - \left[\frac{1}{r} - \frac{1}{4} \pi r (r-1) \hat{v}_{th}^2 \right]^{1/2} \right\}^2. \quad (22)$$

At the beginning of a simulation, for a given value of the gas temperature and a solid's radius, the initial value of the gas

Reynolds number is calculated for the initial position and velocity of the object using equations (5) and (6). If the initial value of Re is smaller than 800, it is necessary to include C_D in equations (10)–(13) as a function of the position and the momentum of a solid. The appropriate functional form of the drag coefficient in such cases is obtained from equations (4), (5), and (6). During the numerical integration of equations (10)–(13), the magnitude of the gas Reynolds number is constantly monitored. If, before the object reaches the location of the maximum density, Re changes its magnitude in such a way that its new value is no longer within its previous range, the integrations are continued with another set of equations (10)–(13), whose drag coefficient has the appropriate functional form for the new range of the gas Reynolds number. The initial conditions for this set of equations are given by the position and velocity of the object at the time that Re changed its range.

We numerically integrated equations (10)–(13) for different values of the gas temperature, solids' radii and densities, and also different values of β . In all our simulations, the objects were initially placed on the x -axis ($\theta = 0$) and were given a Keplerian circular velocity. Figures 2 and 3 show the radial migration of solids ranging from micron-sized particles to 100 m objects initially at 2 AU (inward migration) and 0.25 AU (outward migration) for a gas density given by equation (16) with $\beta = 1$. The densities of the objects are

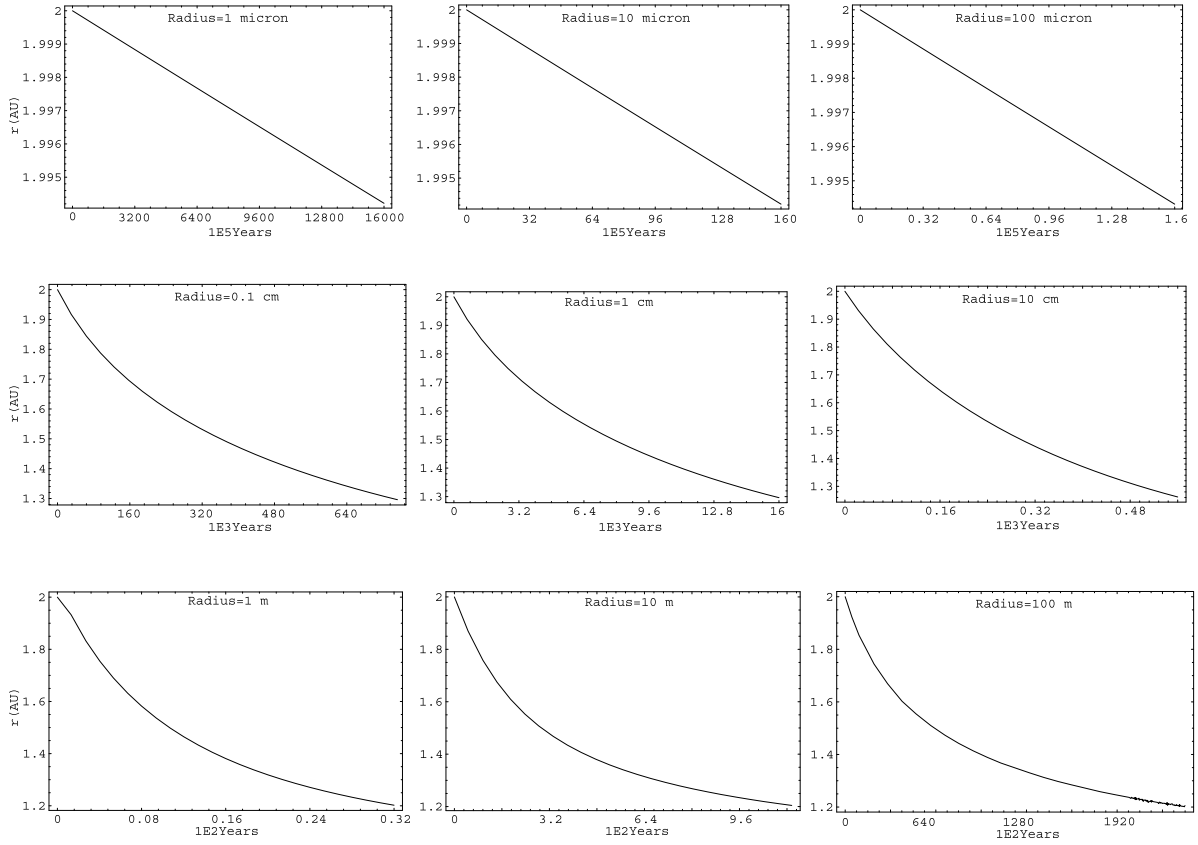


FIG. 2.—Inward migration of solids with radii ranging from $1\ \mu\text{m}$ to $100\ \text{m}$ and densities equal to $2\ \text{g cm}^{-3}$. The disk is isothermal at $1000\ \text{K}$, and its density is given by eq. (16) with $\beta = 1$. Note the different scales on time axes.

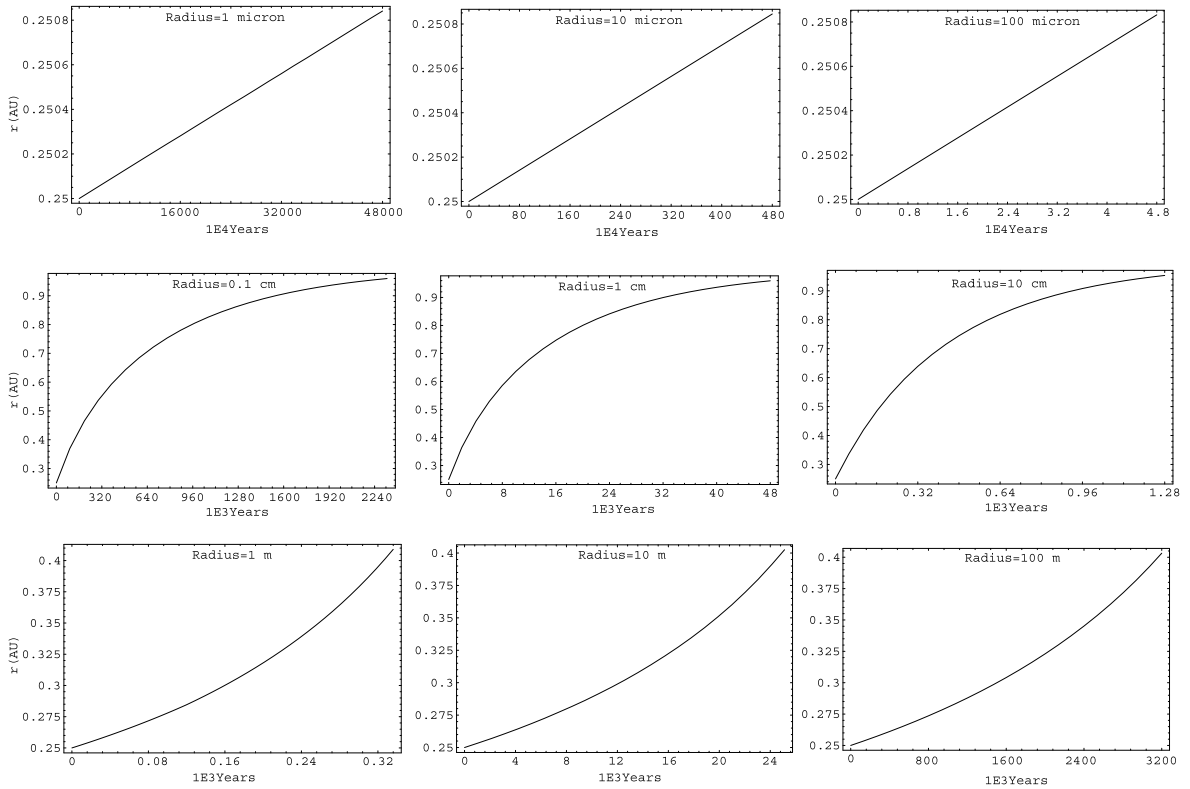


FIG. 3.—Outward migration of solids with radii ranging from $1\ \mu\text{m}$ to $100\ \text{m}$ and densities equal to $2\ \text{g cm}^{-3}$. The disk is isothermal at $1000\ \text{K}$, and its density is given by eq. (16) with $\beta = 1$. Note the different scales on time axes.

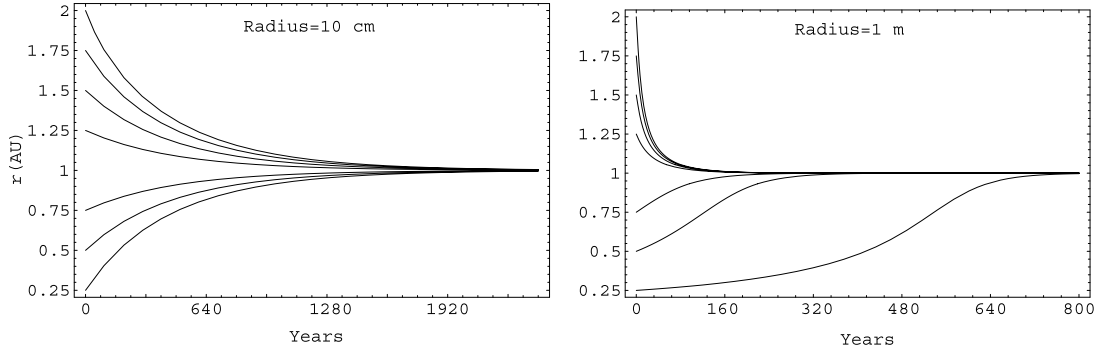


FIG. 4.—Among the solids of Figs. 2 and 3, the ones with 10 cm and 1 m radii undergo rapid migrations. Note the different scales on time axes.

equal to 2 g cm^{-3} . As expected, small particles spend more time with the gas and take longer times to migrate inward/outward. As the sizes of the particles increase, while their densities stay constant, the rate of radial migration also increases. One can see from Figures 2 and 3 that for the abovementioned physical properties of the gas and solids, the graphs of the 10 cm and 1 m objects show the most rapid radial migration, comparable to the timescale of the growth of nonaxisymmetries in disk instability models. Figure 4 shows a comparison of the times of migration for these two cases. Increasing the radius of the solids to 10 m or higher, one observes that the rate of migration decreases again.

Figure 4 also shows that the rates of inward and outward migrations for meter-sized objects at equal distances on both sides of 1 AU are different. The inward migrations starting at 1.75, 1.5, and 1.25 AU occur more rapidly than the outward migrations from 0.25, 0.5, and 0.75 AU. Our simulations indicate similar results for larger objects as well. This can be attributed to the fact that for two identical objects at equal distances on both sides of the maximum of the density, the rate of change of angular momentum of the object given by equation (13), is larger for the farther object. As a result, the angular momentum of this object is decreased more rapidly, which in turn results in its faster approach to the location of the maximum density.

The rate of radial migration also varies with the density of solids. Figure 5 shows the migrations of solids with radii of 10 cm and 10 m for three different values of 1, 2, and 5 g cm^{-3} for the solid's density. The physical properties of the gas in this figure are identical to Figure 2. Our simulations show that the rate of radial migration increases by increasing the solid's density for centimeter-sized and smaller particles, and it decreases for meter-sized and larger objects. The reason for this can be found in the contribution of the drag force (eq. [8]) to the change of the radial and the angular momenta of the solid given by equations (12) and (13). Recall that $\hat{\rho}_g(r)$ is a dimensionless quantity with a numerical value equal to $r_0^3 \rho_g(r) / m_p$. For a constant value of a_p , increasing the density of the object will result in increasing its mass and, consequently, in decreasing the dimensionless density $\hat{\rho}_g(r)$. In case of centimeter-sized and smaller objects, the radial component of the velocity of the solid relative to the gas (i.e., P_r , as given by eqs. [14]) is more dominant than its transverse component, which implies that the effect of decreasing $\hat{\rho}_g(r)$, which from equation (12) results in an increase in the rate of migration of the solid, is larger for larger solids densities. On the other hand, for meter-

sized and larger objects in which the transverse component of the object's relative velocity with respect to the gas is quite large, the decrease in the numerical value of $\hat{\rho}_g(r)$ for higher values of the densities of solids appears largely in the rate of change of the angular momentum of the object given by equation (13). An increase in the object's density results in a smaller absolute value for the rate of change of its angular momentum, which implies that the object becomes more reluctant to lose/gain angular momentum and migrate inward/outward.

Numerical integrations have also been carried out for different values of the temperature of the gas. The effect of a change in temperature appears in the thermal velocity of the gas, which in turn results in changes in the value of the gas viscosity and eventually its drag coefficient, and also affects the pressure gradient and the magnitude of the velocity of

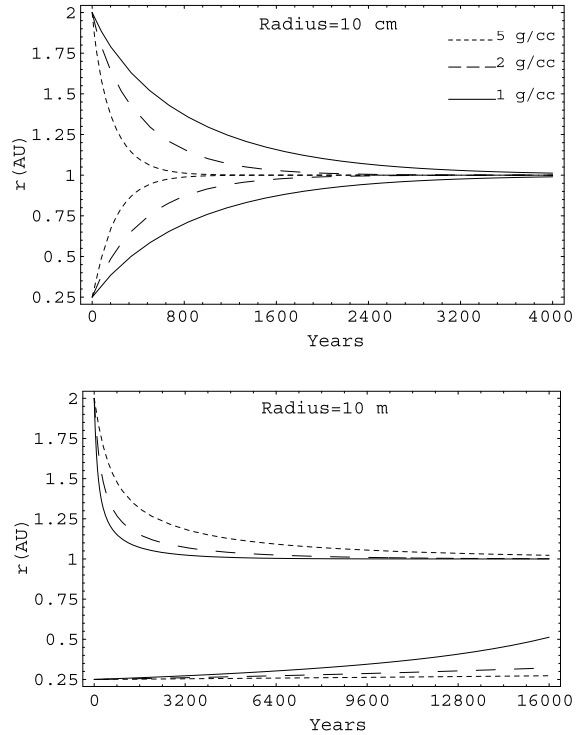


FIG. 5.—Migration of a 10 cm particle and a 10 m object with densities equal to 1, 2, and 5 g cm^{-3} . Note the different scales on time axes.

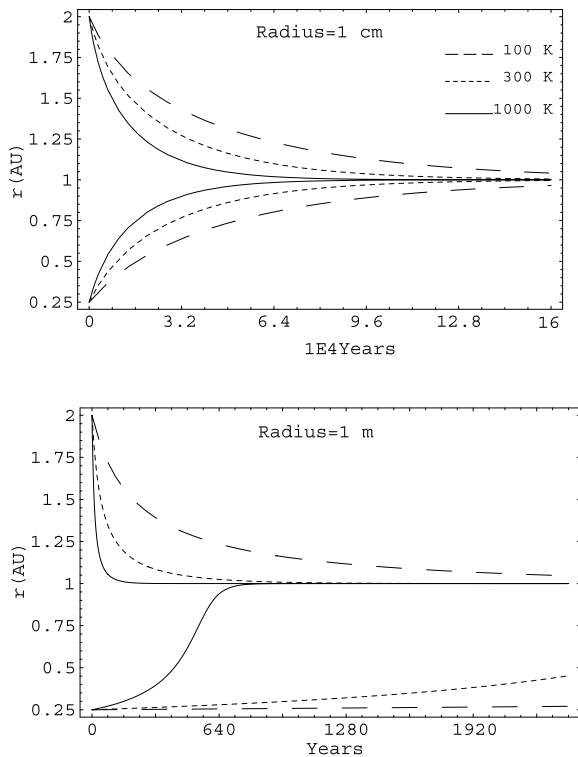


FIG. 6.—Migration of a 1 cm particle (*top*) and a 1 m object (*bottom*) at different temperatures. The densities of both objects are equal to 2 g cm^{-3} . Note the different scales on time axes.

the solids relative to the gas. Figure 6 shows the rates of migrations of a 1 cm particle and a 1 m object for different values of the gas temperature. The densities of both objects are equal to 2 g cm^{-3} and $\beta = 1$. As shown here, the rates of migrations of objects increase by increasing the gas temperature, a familiar result that is a consequence of an increase in the pressure gradient for a higher value of the temperature.

5. SUMMARY AND DISCUSSION

We have studied the motions of small solids in the vicinity of a density enhancement in a rotating nonuniform gaseous disk. We assume that the gas is isothermal and ideal. In this case, an enhancement in the gas density corresponds to a maximum in its pressure. As expected, because of the pressure gradient associated with the radial change of the gas density, solids on both sides of the location of the maximum pressure (or density) undergo inward/outward migrations. We have studied such migrations in a model solar nebula where solids, in addition to the gravitational attraction of the central star, are also subject to gas drag.

In general, the rate of the migration of a solid in a gaseous medium due to the pressure gradient varies with the solid's mass and also with the physical properties of the gas such as

its density and temperature. As shown in § 2, changes in the gas temperature and density will affect the mean thermal velocity and also affect the mean free path of the gas molecules. Such changes show their effects in the drag force of the gas through its Reynolds number and also through the relative velocity of the solid with respect to the gas and result in different rates of migration. An analytical study of the general dependence of the rate of migration of a solid on the physical properties of the solids and the nebular gas is currently underway.

As mentioned earlier, our motivation for initiating this study was to seek the possibility of the application of the results to the formation of planetesimals in marginally gravitationally unstable disk models. As shown by Boss (2000), the disk instability scenario suggests rapid formation of giant gaseous protoplanets followed by sedimentation of small solids at the location of spiral arms and clumps of a gravitationally unstable disk, all in about 1000 yr. In our study, we considered a simple model of the solar nebula in order to focus our attention solely on the times of migration of solids and their variations with physical parameters of the system. Our results indicate that it is indeed possible for solids within certain ranges of size and density to migrate quite rapidly to the locations of maximum values of the gas density. For the model studied here, solids with densities of a few g cm^{-3} , and with radii ranging from several centimeters to a few meters, migrate a radial distance of 1 AU during a time ($\sim 10^3$ yr) comparable with the giant planet formation timescale implied by the disk instability model.

Regardless of whether disk instability can form gas giant planets, the likelihood that the solar nebula was marginally gravitationally unstable implies that the processes studied here may have enhanced the growth rates of solid planetesimals.

In closing, we would like to mention that the calculations in this study have been done for two-dimensional motions and for a solar nebula that may not fully reflect the properties of a more realistic environment. In this study, we focused on the motion of solids as isolated objects without including their mutual interactions. To obtain a better understanding of the dynamics of solids and the times of their migrations, it is necessary to extend such an analysis to a three-dimensional case and to allow for interactions between the objects. It is also important to consider temperature and density distributions for the nebular gas that portray the physical properties of a gravitationally unstable disk in a more realistic way. In a complete treatment of the problem, it is also important to take the gravitational attraction of the nebula into account. Such considerations are currently underway.

We would like to thank the referee, Stu Weidenschilling, for his valuable comments and suggestions. This work is partially supported by the NASA Origins of the Solar System Program under grant NAG5-10547 and by the NASA Astrobiology Institute under grant NCC2-1056.

REFERENCES

- Adachi, I., Hayashi, C., & Nakazawa, K. 1976, *Prog. Theor. Phys.*, 56, 1756
 Boss, A. P. 2000, *ApJ*, 536, L101
 Epstein, P. S. 1924, *Phys. Rev.*, 23, 710
 Iwasaki, K., Tanaka, H., & Emori, H. 2001, *PASJ*, 53, 321
 Kary, D. M., Lissauer, J. J., & Greenzweig, Y. 1993, *Icarus*, 106, 288
 Kennard, E. H. 1938, *Kinetic Theory of Gases* (New York: McGraw-Hill)
 Kiang, T. 1962, *MNRAS*, 123, 359
 Landau, L. D., & Lifshitz, E. M. 1959, *Fluid Mechanics* (London: Pergamon)

- Malhotra, R. 1993, *Icarus*, 106, 264
Pollack, J. B., Hubickyj, O., Bodenheimer, P., Lissauer, J. J., Podlak, M., & Greenzweig, Y. 1996, *Icarus*, 124, 62
Probstein, R. F., & Fassio, F. 1969, *AIAA J.*, 8, 4
Supulver, K. D., & Lin, D. N. C. 2000, *Icarus*, 146, 525
- Weidenschilling, S. J. 1977, *MNRAS*, 180, 57
Weidenschilling, S. J., & Davis, D. R. 1985, *Icarus*, 62, 16
Whipple, F. L. 1964, *Proc. Natl. Acad. Sci.*, 52, 565
———. 1972, in *From Plasma to Planets*, ed. A. Elvius (London: Wiley), 211